Direct Determination of the Bias-Dependent Series Parasitic Elements in SiC MESFETs

S. Manohar, A. Pham, and Nicole Evers

Abstract—We propose a simple and direct extraction procedure for the determination of bias-dependent parasitic resistive elements in SiC MESFETs. This extraction technique is based on a frequency evolution of measured Z-parameters of a metal semiconductor field effect transistor (MESFET) under active bias conditions. Using this method, the equivalent-circuit parameters of an SiC MESFET have been extracted at different bias points, and the variation of the bias-dependent series resistive elements studied. The measured and modeled S-parameters demonstrate a good correlation up to 20 GHz.

Index Terms—Direct extraction, MESFET, SiC, small-signal model.

I. INTRODUCTION

THE need for first-pass design success provides the impetus for the development of accurate device models for use in simulation tools. Modeling FETs using lumped equivalent-circuit approaches usually involves the determination of extrinsic elements, which primarily come from pad contacts, prior to the extraction of intrinsic device parameters. The widely used cold-FET/hot-FET method is based on such a concept. In this method, parasitic elements are determined from S-parameter measurements at zero drain bias, at which the intrinsic model becomes much simpler [1]. However, the determination of parasitic resistance by this method requires *a priori* knowledge of at least one of the resistance (gate, drain, or source) in order to determine the rest of the parasitic elements. Additional measurements are usually employed to extract one of these resistive elements. Otherwise, a partial optimization procedure is used to determine all parasitic elements. Furthermore, conventional modeling techniques assume that source and drain resistance is bias independent. This assumption must be reconsidered in the light of [2]–[4]. From a physical perspective, gate resistance comes from metallization resistance of a gate Schottky contact. However, the source and drain resistance includes contact resistance, as well as any bulk resistance leading up to an active channel. Changes in gate and drain voltage cause fluctuation in width of the lateral depletion layer, effectively increasing or decreasing bulk resistance. To date, dc measurement techniques [3], [5] have been
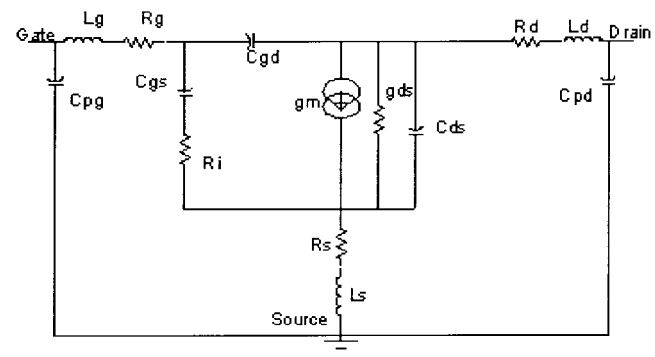
S. Manohar and A. Pham are with the Department of Electrical and Computer Engineering, University of California at Davis, Davis, CA 95616-5294 USA.

N. Evers is with the General Electric Corporate Research and Development Center, Schenectady, NY 12301 USA.

Fig. 1. Topology of the equivalent-circuit model of a 500 μm $\times$ 0.6 μm SiC MESFET.

proposed to determine bias-dependent source and drain resistance, but these methods require the characterization of FETs of different gate lengths. Recently, Sommer demonstrated the extraction of bias-dependent source resistance using active-bias measurements, but the method requires partial optimization [6]. Modified pinched cold-FET techniques [7], [8] have also been proposed, but the variation of parasitic elements with drain bias cannot be obtained.

In this paper, we present a simple series extrinsic element extraction scheme in which parasitic elements are determined by equating measured Z-parameters with equivalent analytic expressions. These analytic expressions are derived specifically for an SiC MESFET equivalent-circuit model that incorporates the charging resistance. Using this method, the bias-dependent (both on gate and drain voltage) series drain and source resistance can be directly extracted using measured active-bias S-parameters. The measured and modeled S-parameters demonstrate a good correlation up to 20 GHz.

II. THEORETICAL ANALYSIS

Based on the equivalent-circuit model of a MESFET (Fig. 1), Y-parameters of the intrinsic MESFET are given by [9]

$$Y_{11} = \frac{R_i C_{gs}^2 \omega^2}{D} + j\omega \left(\frac{C_{gs}}{D} + C_{gd} \right) \tag{1}$$

$$Y_{21} = g_{mo} - j\omega C_{gd} \tag{2}$$

$$Y_{12} = -j\omega C_{gd} \tag{3}$$

$$Y_{22} = g_{ds} + j\omega \left(C_{ds} + C_{gd} \right) \tag{4}$$

where $D = 1 + R_i^2 C_{gs}^2 \omega^2$ and $g_{mo} = g_m e^{(-j\omega\tau)}$.

From (1)–(4), $(Y_{11}Y_{22} - Y_{12}Y_{21})$ can be calculated and rearranged as

$$
\begin{aligned}
Y_{11}&Y_{22} - Y_{12}Y_{21} \\
&= \frac{\omega^2 \left(R_i C_{gs}^2 g_{ds} - C_{gs}C_{ds} - C_{gs}C_{gd} \right)}{D} - \omega^2 C_{gd}C_{ds} \\
&+ \frac{j\omega^3 \left[R_i C_{gs}^2 (C_{ds} + C_{gd}) + R_i^2 C_{gs}^2 g_{ds}C_{gd} \right]}{D} \\
&+ \frac{j\omega \left[C_{gd}g_{mo} + (C_{gs} + C_{gd})g_{ds} \right]}{D}.
\end{aligned}
\tag{5}
$$

The following manipulations are performed to simplify (5).
1) The first term of the imaginary part of $Y_{11}Y_{22} - Y_{12}Y_{21}$ is multiplied and divided by R_i.
2) $(C_{ds} + C_{gd})$ and $g_{ds}C_{gd}$ are added and subtracted from the numerator of the first two terms of the imaginary part of $Y_{11}Y_{22} - Y_{12}Y_{21}$.
3) The imaginary part of $Y_{11}Y_{22} - Y_{12}Y_{21}$ is rearranged in terms of D where necessary.

The imaginary part of (5) reduces to

$$
\begin{aligned}
\text{Im}&(Y_{11}Y_{22} - Y_{12}Y_{21}) \\
&= j\omega \left[\frac{(C_{ds}+C_{gd})D}{R_i D} - \frac{(C_{gd}+C_{ds})}{R_i D} + \frac{g_{ds}C_{gd}D}{D} - \frac{g_{ds}C_{gd}}{D} \right] \\
&+ j\omega \left[\frac{\left(C_{gd}g_{mo} + (C_{gs}+C_{gd})g_{ds} \right)}{D} \right].
\end{aligned}
\tag{6}
$$

Since $R_i^2 C_{gs}^2 \omega^2 < 0.01$ below 10 GHz, $D = 1 + R_i^2 C_{gs}^2 \omega^2$ can be approximated to be $D \cong 1$. Thus, (5) becomes

$$
\begin{aligned}
Y_{11}&Y_{22} - Y_{12}Y_{21} \\
&= \omega^2 \left(R_i C_{gs}^2 g_{ds} - C_{gs}C_{ds} - C_{gs}C_{gd} - C_{gd}C_{ds} \right) \\
&+ j\omega \left[C_{gd}g_{mo} + (C_{gs} + C_{gd})g_{ds} \right].
\end{aligned}
\tag{7}
$$

Converting Y-parameters to Z-parameters, adding the series parasitic elements, and simplifying the resulting expressions, the analytic expressions for the imaginary part of the Z-parameters of the MESFET reduce to [10]

$$
\frac{1}{\omega}\text{Im}(Z_{11}) = L_s + L_g - \frac{\omega^2 E_g - F_g}{\omega^2(\omega^2 + B)}
\tag{8}
$$

$$
\frac{1}{\omega}\text{Im}(Z_{12}) = L_s - \frac{E_{s1}}{\omega^2 + B}
\tag{9}
$$

$$
\frac{1}{\omega}\text{Im}(Z_{12}) = L_s - \frac{\omega^2 E_{s2} - F_{s2}}{\omega^2(\omega^2 + B)}
\tag{10}
$$

$$
\frac{1}{\omega}\text{Im}(Z_{22}) = L_d + L_s - \frac{E_d}{\omega^2 + B}
\tag{11}
$$

where L_s, L_g, and L_d are the source, gate, and drain inductances, respectively, and F_g, E_g, E_{s1}, E_{s2}, F_{s2}, E_d, and B are the constants. Since the approximation $D \approx 1$ is valid only in the low-frequency regime, the parasitic inductive elements are extracted from the measured Z-parameters below 10 GHz. Assuming that the extrinsic parasitic elements are constant with respect to frequency, their values determined

from Z-parameters below 10 GHz can be used at higher frequency ($>$10 GHz) for intrinsic parameter extraction. Using linear regression techniques and (8)–(11), the extrinsic gate, source, and drain inductances can be extracted.

In order to determine the bias-dependent source and drain resistance, the following equations are derived from (1)–(4):

$$
Z_{12} - R_s - j\omega L_s = \frac{-Y_{12}}{Y_{11}Y_{22} - Y_{12}Y_{21}}
\tag{12}
$$

$$
Z_{21} - R_s - j\omega L_s = \frac{-Y_{21}}{Y_{11}Y_{22} - Y_{12}Y_{21}}.
\tag{13}
$$

From (12) and (13), we obtain

$$
\frac{j\omega C_{gd}}{Z_{12} - R_s - j\omega L_s} = \frac{-g_{mo} + j\omega C_{gd}}{Z_{21} - R_s - j\omega L_s}.
\tag{14}
$$

Equating the real and imaginary parts of (14), we get

$$
\begin{aligned}
\left[\frac{\text{Im}(Z_{12})}{\omega} \right] &= \frac{C_{gd}}{g_m} \Big\langle \big\{ \text{Sin}(\omega\tau)\left[\text{Im}(Z_{21}) - \text{Im}(Z_{12}) \right] \big\} \\
&+ \big\{ \text{Cos}(\omega\tau)\left[\text{Re}(Z_{12}) - \text{Re}(Z_{21}) \right] \big\} \Big\rangle + L_s
\end{aligned}
\tag{15}
$$

$$
\begin{aligned}
\left[\text{Re}(Z_{12}) \right] &= \frac{C_{gd}}{g_m}\omega \Big\langle \big\{ \text{Cos}(\omega\tau)\left[\text{Im}(Z_{21}) - \text{Im}(Z_{12}) \right] \big\} \\
&- \big\{ \text{Sin}(\omega\tau)\left[\text{Re}(Z_{12}) - \text{Re}(Z_{21}) \right] \big\} \Big\rangle + R_s.
\end{aligned}
\tag{16}
$$

Since the real part of Y_{12} is zero [see (3)], the computed Y_{12} from the Z-parameters can be set to zero to find R_d, shown in (17), at the bottom of the following page, where

$$
\begin{aligned}
&\begin{bmatrix} Z_{11}^{int} & Z_{12}^{int} \\ Z_{21}^{int} & Z_{22}^{int} \end{bmatrix} \\
&= \begin{bmatrix} Z_{11} & Z_{12} \\ Z_{21} & Z_{22} \end{bmatrix} \\
&- \begin{bmatrix} R_s + R_g + j\omega(L_s + L_g) & R_s + j\omega L_s \\ R_s + j\omega L_s & R_s + j\omega(L_s + L_d) \end{bmatrix}.
\end{aligned}
$$

III. EQUIVALENT-CIRCUIT PARAMETER (ECP) EXTRACTION PROCEDURE

500 μm $\times$ 0.6 μm SiC MESFETs are used in the extraction procedure. On-wafer S-parameter measurements are performed using a Cascade Microtech probe station, an HP 8510C network analyzer, and HP 6634 and HP 3531 dc sources. Prior to S-parameter measurements, an on-wafer line-reflect-match (LRM) calibration is performed to result in reference planes at the edge of probe tips. S-parameters of the pinched-off device ($V_d = 0$ and $V_{gs} < V_t$) are first taken, and are converted to equivalent admittance parameters to determine the parasitic pad capacitors [1]. The gate resistance is extracted by a cold-FET method [7] and is held constant throughout the
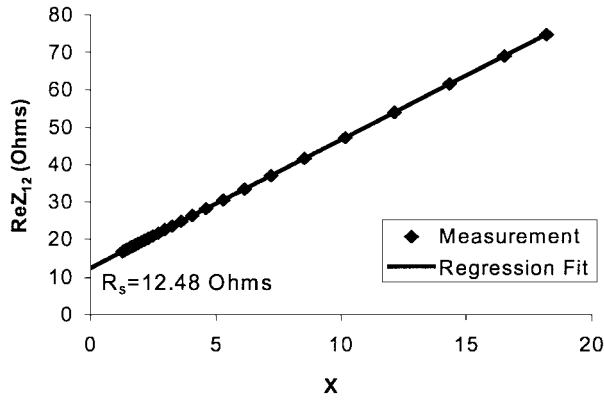
Fig. 2. Illustration of the linear regression technique to determine the source resistance. The source resistance is determined from the intercept to be 12.48 Ω. $X = \omega\langle\{\mathrm{Cos}(\omega\tau)[\mathrm{Im}(Z_{21}) - \mathrm{Im}(Z_{12})]\} - \{\mathrm{Sin}(\omega\tau)[\mathrm{Re}(Z_{12}) - \mathrm{Re}(Z_{21})]\}\rangle * 10^{-12}$.

extraction process. Next, S-parameters of the SiC MESFET biased at $V_d = 30$ V and $V_{gs} = -4.5$ are measured, and are converted to Y-parameters. The pad capacitor responses in active-bias Y_{11} and Y_{22} are deembedded using the extracted pad capacitor values obtained from cold-FET measurements. The Y-parameters are then converted to Z-parameters, which are equivalent to the analytic formulations [see (8)–(11)]. Using (8)–(11) and linear regression techniques [10], the gate, source, and drain inductors are determined prior to the determination of bias-dependent source and drain resistance.

The next step is to determine bias-dependent source and drain resistance using Z-parameters. In this step, τ must be determined prior to the extraction of the source resistance. First, the slope of (15) is determined using the linear regression technique with an initial estimate of τ. The value of τ is then iterated until the slopes of (15) and (16) are identical. Once τ is known, the bias-dependent source resistance can be determined from the intercept of linear regression of (16), as shown in Fig. 2. Once the source resistance is determined, the drain resistance can be calculated by setting $\mathrm{Re}(Y_{12})$ to zero [see (17)]. After the extraction of the extrinsic elements, the intrinsic parameters can be calculated from hot-FET measurements [9]. The values of the ECPs are summarized below in Tables I and II.

IV. RESULTS AND DISCUSSION

Fig. 3 shows an excellent agreement between measured and modeled S-parameters up to 20 GHz. The experimental results verify the validity of the developed extraction technique to determine small-signal extrinsic elements. S-parameters are taken at different drain and gate voltage to determine bias-dependent extrinsic elements. Using the method outlined above, both drain and source series resistance is determined as a function of bias points. Figs. 4 and 5 demonstrate the extracted drain and source

TABLE I
INTRINSIC ELEMENTS OF SiC MESFET (1–20 GHz) ($V_{ds} = 30$ V, $V_{gs} = -4.5$ V)

Gate width	g_m (ms)	Γ (psec)	$R_{ds}(\Omega)$	C_{gs}(pF)	C_{ds}(pF)	C_{gd}(pF)	R_i (Ω)
500 μ m	10.63	5.7	1030	0.151	0.0707	0.028	10.6

TABLE II
EXTRINSIC ELEMENTS OF SiC MESFET (1–20 GHz)

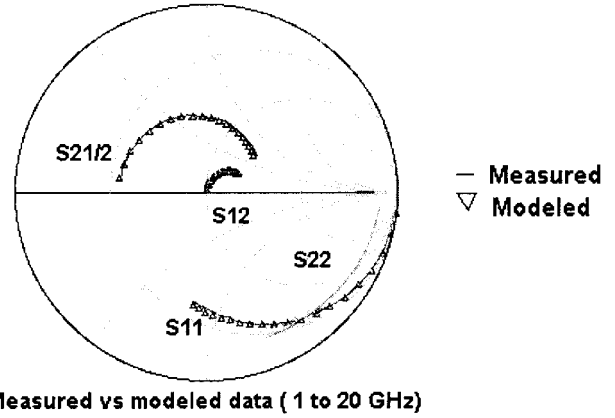| Gate width	L_g(nH)	L_d(nH)	L_s(nH)	$R_g(\Omega)$	$R_d(\Omega)$	$R_s(\Omega)$	C_{pg}(pF)	C_{pd}(pF)
500 μ m	0.034	0.023	0.00	6.7	2.075	12.48	0.0033	0.0099

Fig. 3. Agreement between measured and modeled S-parameters from 1 to 20 GHz ($V_{ds} = 30$ V, $V_{gs} = -4.5$ V). One may notice that S_{21} is less than one, which results from a mismatch between a 50-Ω network analyzer and the high input impedance of SiC MESFETs.
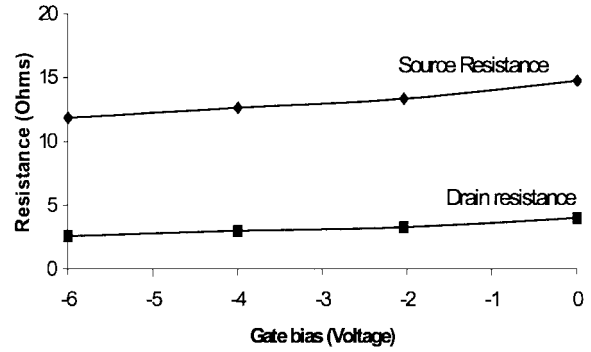

Fig. 4. Extracted extrinsic bias-dependent source and drain resistance at a drain voltage of 30 V and gate biases of -8, -6, -4, -2, and 0 V.

resistance as a function of drain and gate voltage. Since the extrinsic series inductors arise primarily from the metal pads, their inductance values are independent of applied bias. For the same reason, gate resistance is also bias independent. One may observe from Fig. 4 that the source and drain resistance increases with the rise of gate voltage for a fixed drain voltage. A decrease in gate voltage will enlarge the width of the lateral depletion region. As the width of the lateral depletion region increases,

$$R_d = \frac{\mathrm{Im}(Z_{12}^{\mathrm{int}})\left[\mathrm{Im}\big(Z_{11}^{\mathrm{int}}Z_{22}^{\mathrm{int}} - Z_{12}^{\mathrm{int}}Z_{21}^{\mathrm{int}}\big)\right] + \mathrm{Re}(Z_{12}^{\mathrm{int}})\left[\mathrm{Re}\big(Z_{11}^{\mathrm{int}}Z_{22}^{\mathrm{int}} - Z_{12}^{\mathrm{int}}Z_{21}^{\mathrm{int}}\big)\right]}{\mathrm{Im}(Z_{12}^{\mathrm{int}})\mathrm{Im}(Z_{11}^{\mathrm{int}}) + \mathrm{Re}(Z_{12}^{\mathrm{int}})\mathrm{Re}(Z_{11}^{\mathrm{int}})} \tag{17}$$
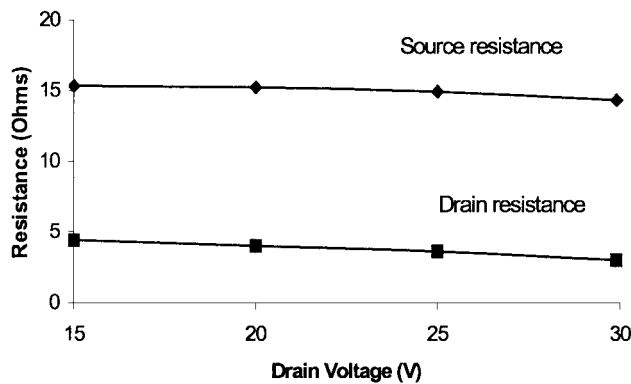
Fig. 5.   Extracted extrinsic bias-dependent source and drain resistance at a gate voltage of −4 V and drain biases of 15, 20, 25, and 30 V.

the distance between the depletion region and the source/drain ends of the channel decreases. Since the source and drain resistance is defined to be the sum of the pad contact resistance and the bulk resistance up to the edge of the gate depletion region, the extracted bias-dependent source and drain resistance is consistent with the previously described physical behavior. From Fig. 5, one may notice that the drain resistance decreases with an increase in bias. This can be attributed to the increase in the lateral depletion width on the drain side with the rise in drain voltage. The slight changes of the source resistance would rather be attributed to the variation of field-dependent mobility than the changes of the lateral depletion width [2].

V. Conclusions

We have demonstrated a simple technique to directly extract the extrinsic elements of an SiC MESFET. This method requires only the S-parameters measured at zero drain voltage and a gate voltage below pinchoff and at a bias point in saturation. The developed method enables the extraction of extrinsic bias-dependent drain and source resistance. The validity of the ECP extraction procedure can be verified from the excellent agreement between measured and modeled S-parameters up to 20 GHz.

References

[1] G. D. Dambrine, A. Cappy, F. Helidore, and E. Playez, "A new method for determining the FET small-signal equivalent circuit," *IEEE Trans. Microwave Theory Tech.*, vol. 36, pp. 1151–1159, July 1988.

[2] Y. T. Tsai and T. A. Grotjuhn, "Source and drain resistance studies of short-channel MESFETs using two-dimensional device simulators," *IEEE Trans. Electron Devices*, vol. 37, pp. 775–780, Mar. 1990.

[3] Y. H. Byun, M. S. Shur, A. Peczalski, and F. L. Schuermeyer, "Gate-voltage dependence of source and drain series resistances and effective gate length in GaAs MESFET's," *IEEE Trans. Electron Devices*, vol. 35, pp. 1241–1246, Aug. 1988.

[4] J. M. Golio, *Microwave MESFET's and HEMTs.* Norwood, MA: Artech House, 1991.

[5] L. Selmi, R. Menozzi, P. Gandolfi, and B. Ricco, "Numerical analysis of the gate voltage dependence of the series resistances and effective channel length in submicrometer GaAs MESFET's," *IEEE Trans. Electron Devices*, vol. 39, pp. 2015–2020, Sept. 1992.

[6] V. Sommer, "A new method to determine the source resistance of FET from measured S-parameters under active-bias condition," *IEEE Trans. Microwave Theory Tech*, vol. 43, pp. 504–510, Mar. 1995.

[7] R. Tayrani, J. E. Gerber, T. Daniel, R. S. Pengelly, and U. L. Rohde, "A new and reliable direct parasitic extraction method for MESFET's and HEMT's," in *23th Eur. Microwave Conf.*, Tunbridge Wells, U.K., Sept. 1993, pp. 451–453.

[8] C.-H. Kim, K.-S. Yoon, J.-W. Yang, J.-H. Lee, C.-S. Park, J.-J. Lee, and K.-E. Pyun, "A new extraction method to determine bias-dependent source series resistance in GaAs FETs," *IEEE Trans. Microwave Theory Tech.*, vol. 46, pp. 1242–1250, Sept. 1998.

[9] C. F. Campbell and S. A. Brown, "An analytical method to determine GaAs FET parasitic inductances and drain resistance under active bias conditions," *IEEE Trans. Microwave Theory Tech.*, vol. 49, pp. 1241–1247, July 2001.

[10] J. P. Raskin, G. Dambrine, and R. Gillon, "Direct extraction of the equivalent circuit parameters for the small signal SOI MOSFET's," *IEEE Microwave Guided Wave Lett.*, vol. 7, pp. 408–410, Dec. 1997.

[11] J. A. Raskin-Hernandez, J. Apolinar, F. E. Rangel-Patino, F. Elias, and J. Perdomo, "Full RF characterization for extracting the small-signal equivalent circuit in microwave FET's," *IEEE Trans. Microwave Theory Tech.*, vol. 44, pp. 2625–2633, Dec. 1996.

[12] J. P. Raskin, R. Gillon, J. Chen, D. Vanhoenacker-Janvier, and J. P. Colinge, "Accurate SOI MOSFET characterization at microwave frequencies for device performance optimization and analog modeling," *IEEE Trans. Electron Devices*, vol. 45, pp. 1017–1025, May 1998.

S. Manohar, photograph and biography not available at time of publication.

A. Pham, photograph and biography not available at time of publication.

Nicole Evers, photograph and biography not available at time of publication.